Permutation Channel Modulation: New Index Modulation Mechanism for MIMO

Rahmat Faddli Siregar, Nandana Rajatheva, and Matti Latva-aho
Centre for Wireless Communications, University of Oulu, Finland
E-mail: rahmat.siregar@oulu.fi, nandana.rajatheva@oulu.fi, matti.latva-aho@oulu.fi

2021 IEEE 93rd Vehicular Technology Conference (VTC2021-Spring) | 978-1-7281-8964-2/20/$31.00 ©2021 IEEE | DOI: 10.1109/VTC2021-Spring51267.2021.9448790

***Abstract*—In this paper, we propose a novel index modulation mechanism called permutation channel modulation (PCM) by exploiting spatial resource of multiple input multiple output (MIMO). A set of permutation matrices is treated as indices to convey information bits by modulating a block of bits to a permutation matrix. Assuming that channel state information at transmitter (CSIT) is known, modulated permutation matrix is multiplied to the singular values of MIMO channel matrix obtained from decomposing the channel matrix using singular values decomposition (SVD). Besides to a permutation matrix, information bits are also modulated to constellation symbols. Therefore, the transmitted signals contain two sources of information: a permutation matrix and constellation symbols. At the receiver, transmitted symbols and a permutation matrix are detected using our proposed detection scheme. We derive the capacity expression and define the optimal capacity by finding the optimal power allocation at each transmission. As performance measure, capacity of PCM is compared with existing techniques. Using 4×4, we find that the capacity of PCM is doubled and remains superior with higher antenna settings. Our work creates a new paradigm of index modulation for multiple antenna transmissions by exploiting its spatial resource and significantly improves the capacity and outage probability performances.**

***Index Terms*—PCM, MIMO, permutation matrix, SVD**

I. Introduction

The exploitation of multiple input multiple output (MIMO) has broadened the alternatives for wireless system transmission. Conventional MIMO scheme has been developed into numerous scenarios and available in existing literature [1]–[4]. Recently, many works is introduced since the presence of MIMO especially to investigate the benefits of its spatial resource, e.g. spatial modulation (SM) [5]–[8], quadrature spatial modulation (QSM) [9]–[13], etc. The fundamental idea of these new techniques is to discover alternative indices to convey information bits other than the conventional way, i.e., constellation symbols. Many advantages are offered such as high compatibility to existing MIMO scheme, high spectral efficiency and free of inter-channel interference [14].

At the beginning, SM is proposed to modulate a single antenna by treating the antenna as modulated index to convey information bits along with a constellation symbol. The technique is effective to avoid inter-channel interference with low complexity receiver [5]. On the other hand, SM decreases the achievable rate of conventional MIMO since it only activates one antenna per transmission. Furthermore, SM requires twice number of transmit antennas to increase one bit since it is bounded to have 2^n transmit antennas. A new technique called generalized spatial modulation (GSM) is then introduced to overcome this issue. It relaxes SM's limitation so that any number of transmit antennas is applicable [15]. However, some advantages of SM are no longer maintained such as its freedom of inter-channel interference. One of the most recent works on index modulation is QSM. The system independently transmits the real and imaginary constellation symbol. Further, it also modulates the activated transmit antennas as information bits [9]. QSM was a breakthrough due to its ability to remove inter-channel interference while conveying higher amount of bits compared to conventional SM. Recently, QSM has also been developed to work in millimeter wave (mmWave) channels [12]. Despite its benefits, receiver complexity grows exponentially with the increase of number of antennas since it employs maximum likelihood (ML) receiver. Furthermore, compared to existing conventional MIMO in [16], number of possible conveyed bits of QSM is lower. Recently, a research on spatial permutation modulation (SPM) for MIMO systems has been published in [7]. The idea is to modulate information bits to a permutation vector and to activate the transmit antenna at consecutive time instants. SPM disperses data along with the time coordinate so that it achieves higher diversity, thus lower error rate. The technique can be applied to various index modulation scenarios such as SM, space-time block coded spatial modulation (STBC-SM) and QSM. However, its contribution to increase achievable rate is inferior [7]. In this paper, we propose a novel index modulation mechanism called permutation channel modulation (PCM) to exploit spatial resource of MIMO by modulating a permutation matrix to convey extra information bits. A permutation matrix is selected and modulated based on the random incoming information bits along with constellation symbols. The modulated permutation matrix is employed to rearrange the singular values by multiplying the modulated permutation matrix to the singular values matrix. A precoded vector resulted from multiplying unitary, modulated permutation, singular values matrices and modulated symbol vector is transmitted over MIMO channel. At the receiver, inter-channel interference is canceled by performing post-processing. The received signal contains two sources of information to be decoded. At first, the permutation matrix is detected. Then by using the detected permutation matrix, transmitted symbols are also detected.

In this paper, our contributions are follows: we derive capacity expression of PCM. Furthermore, optimal power allocation

is also investigated. Capacity of PCM is evaluated and compared with conventional MIMO and mmWave QSM studied in [12]. It is shown that PCM's performance is superior to the others. The behavior of PCM's capacity in antenna enhancement is also studied. PCM obtains greater capacity gain as the number of antennas is enhanced. Moreover, outage probability of PCM is presented and compared with conventional MIMO as well. We find that increasing either number of transmit or receive antennas or both improves the outage probability greater than MIMO. Lastly, simulation result of bit error rate (BER) is discussed. We present various antenna settings and modulation levels using the proposed detection scheme. The result indicates that increasing channel rank or modulation level gives a poorer performance where higher channel rank results worse BER.

The rest of the paper is organized as follows: section II presents the proposed system. Capacity analysis is presented in section III. Results and discussion is provided in section IV. Finally, we conclude the paper in section V.

Notation: In the following, uppercase bold letters **A** denote matrices and lowercase bold letters **a** denote column vectors (unless specified otherwise). $(.)^T$, $(.)^H$, $|.|$, det(.), $E[.]$ denote transpose, Hermitian transpose, absolute value, determinant and expectation of a random variable, respectively.

II. Proposed System

Our proposed system model is depicted in Fig. 1. We propose a novel modulation scheme by modulating a set of permutation matrices to convey information bits along with phase shift keying (PSK) symbols in MIMO system. Perfect channel state information (CSI) at transceiver is assumed to be known so that the MIMO channel matrix can be decomposed using SVD. A precoder is constructed by employing the selected permutation matrix and the property of SVD. At the receiver, the permutation matrix and PSK symbols are detected. We define set $\mathcal{N} \in \{1,...,N\}$ of transmit antennas, $\mathcal{M} \in \{1,...,M\}$ of receive antennas, $\mathcal{S} \in \{s_1,...,s_Q\}$ of Q-level PSK modulated symbols where Q is the modulation level, and $\mathcal{P} \in \{\mathbf{P}_1,...,\mathbf{P}_R\}$ of permutation matrix.

A. Transmitter

First, input bits are divided into two blocks; a block of length $a = p\log_2(Q)$ is modulated and allocated to vector $\mathbf{s} = (s_1,...,s_p : s_i \in \mathcal{S}\ \forall i)^T$ where $p = \min(N,M)$. Element in vector $\mathbf{s}$ indicates the position of modulated symbols that corresponds to its transmit antenna. The second block of length $b = \lfloor \log_2(p!) \rfloor$ is utilized to select permutation matrix $\mathbf{P} \in \mathcal{P}$ of length $p \times p$. Index $R = 2^b$ in set $\mathcal{P}$ is the number of required unique permutation matrices to modulate input bits in the second block. $\mathbf{P}_i = (\mathbf{e}_{\pi(1)},...,\mathbf{e}_{\pi(p)} : \mathbf{e}_{\pi(j)} \in \{\mathbf{e}_1,...,\mathbf{e}_p\})^T$ is the i-th permutation matrix in set $\mathcal{P}$ where $\mathbf{e}_j$ is defined as standard basis row vector of length p where the j-th element is equal to 1 and 0 otherwise. As an example, set of permutation matrices for $N = 3$ and $M = 3$ is shown in TABLE I. For a particular 3×3 setting, a total of six possible combinations of unique permutation matrices are there. However, for binary transmission, only four matrices will be employed. By doing so, the selection of modulated symbols and permutation matrix are independent of each other. Thus, the total transmitted bits at each transmission using the proposed system is

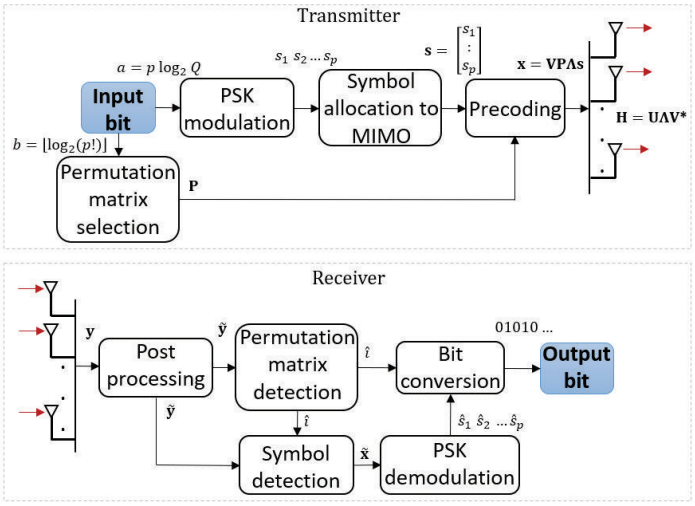

Fig. 1: Proposed system model

$$m = a + b. \tag{1}$$

Next step is to formulate a precoder before sending the signal through MIMO channel. Assume that the antenna array is separated wide enough such that antennas are independent of each other and therefore gives a rank p MIMO channel matrix $\mathbf{H}$ and uncorrelated noise. Matrix

$$\mathbf{H} = \mathbf{U\Lambda V}^* = \begin{bmatrix} u_{1,1} & \dots & u_{1,N} \\ \vdots & \ddots & \vdots \\ u_{M,1} & \dots & u_{M,N} \end{bmatrix} \begin{bmatrix} \lambda_1 & 0 & \dots & 0 \\ 0 & \lambda_2 & \dots & 0 \\ \vdots & \vdots & \ddots & \vdots \\ 0 & 0 & \dots & \lambda_N \end{bmatrix} \begin{bmatrix} v_{1,1} & \dots & v_{1,N} \\ \vdots & \ddots & \vdots \\ v_{N,1} & \dots & v_{N,N} \end{bmatrix}^*, \quad N \le M \tag{2}$$

$$= \begin{bmatrix} u_{1,1} & \dots & u_{1,M} \\ \vdots & \ddots & \vdots \\ u_{M,1} & \dots & u_{M,M} \end{bmatrix} \begin{bmatrix} \lambda_1 & 0 & \dots & 0 \\ 0 & \lambda_2 & \dots & 0 \\ \vdots & \vdots & \ddots & \vdots \\ 0 & 0 & \dots & \lambda_M \end{bmatrix} \begin{bmatrix} v_{1,1} & \dots & v_{1,M} \\ \vdots & \ddots & \vdots \\ v_{N,1} & \dots & v_{N,M} \end{bmatrix}^*, \quad N > M$$

is decomposed using SVD resulting in three matrices where $\mathbf{U}$ and $\mathbf{V}$ are unitary matrices and $\mathbf{\Lambda}$ is a diagonal matrix containing singular values of $\mathbf{H}$ that represents the channel gain of each antenna link. We assume that $\lambda_1 > \lambda_2 > ... > \lambda_p > 0$. At the transmitter, the signal is precoded as

$$\mathbf{x} = \mathbf{VP\Lambda s}. \tag{3}$$

B. Receiver

Signal vector $\mathbf{x}$ is then transmitted and multiplied with MIMO channel $\mathbf{H}$ and the received signal is given as

$$\mathbf{y} = \mathbf{Hx} + \mathbf{n} = (\mathbf{U\Lambda V}^*)\mathbf{VP\Lambda s} + \mathbf{n} = \mathbf{U\Lambda P\Lambda s} + \mathbf{n} \tag{4}$$

where $\mathbf{n} \sim \mathcal{CN}(\mathbf{0}, \mathbf{K_n})$ is i.i.d Gaussian noise vector and $\mathbf{K_n}$ is noise covariance. Received signal vector $\mathbf{y}$ is normalized at the

TABLE I: bits to permutation matrix for 3×3 MIMO

input bits	i	$\mathbf{P}_i$
00	1	$\mathbf{P}_1 = \begin{bmatrix} \mathbf{e}_{\pi(1)} \\ \mathbf{e}_{\pi(2)} \\ \mathbf{e}_{\pi(3)} \end{bmatrix} = \begin{bmatrix} \mathbf{e}_1 \\ \mathbf{e}_2 \\ \mathbf{e}_3 \end{bmatrix} = \begin{bmatrix} 1 & 0 & 0 \\ 0 & 1 & 0 \\ 0 & 0 & 1 \end{bmatrix}$
01	2	$\mathbf{P}_2 = \begin{bmatrix} \mathbf{e}_{\pi(1)} \\ \mathbf{e}_{\pi(2)} \\ \mathbf{e}_{\pi(3)} \end{bmatrix} = \begin{bmatrix} \mathbf{e}_1 \\ \mathbf{e}_3 \\ \mathbf{e}_2 \end{bmatrix} = \begin{bmatrix} 1 & 0 & 0 \\ 0 & 0 & 1 \\ 0 & 1 & 0 \end{bmatrix}$
10	3	$\mathbf{P}_3 = \begin{bmatrix} \mathbf{e}_{\pi(1)} \\ \mathbf{e}_{\pi(2)} \\ \mathbf{e}_{\pi(3)} \end{bmatrix} = \begin{bmatrix} \mathbf{e}_2 \\ \mathbf{e}_1 \\ \mathbf{e}_3 \end{bmatrix} = \begin{bmatrix} 0 & 1 & 0 \\ 1 & 0 & 0 \\ 0 & 0 & 1 \end{bmatrix}$
11	4	$\mathbf{P}_4 = \begin{bmatrix} \mathbf{e}_{\pi(1)} \\ \mathbf{e}_{\pi(2)} \\ \mathbf{e}_{\pi(3)} \end{bmatrix} = \begin{bmatrix} \mathbf{e}_2 \\ \mathbf{e}_3 \\ \mathbf{e}_1 \end{bmatrix} = \begin{bmatrix} 0 & 1 & 0 \\ 0 & 0 & 1 \\ 1 & 0 & 0 \end{bmatrix}$

receiver by multiplying matrix $\mathbf{U}^*$. Note that $\mathbf{V}^*\mathbf{V} = \mathbf{U}^*\mathbf{U} = \mathbf{I}$ as the property of unitary matrices.

$$\tilde{\mathbf{y}} = \mathbf{U}^*\mathbf{y} = \mathbf{U}^*\mathbf{U}\mathbf{\Lambda}\mathbf{P}\mathbf{\Lambda}\mathbf{s} + \mathbf{U}^*\mathbf{n} = \mathbf{\Lambda}\mathbf{P}\mathbf{\Lambda}\mathbf{s} + \tilde{\mathbf{n}}. \tag{5}$$

Multiplying $\mathbf{U}^*$ to vector $\mathbf{y}$ does not change the noise statistics since $\mathbf{U}$ is a unitary matrix. It also cancels inter-channel interference between all antennas. Vector $\tilde{\mathbf{y}}$ is utilized to detect both permutation matrix and transmitted symbols. At first, permutation matrix is detected as

$$\hat{i} = \arg\max_i \left[(\mathbf{P}_i\mathbf{\Lambda}\mathbf{1})^T \, \mathrm{abs}(\mathbf{\Lambda}^{-1}\tilde{\mathbf{y}}) \right], \quad i \in \{1, ..., R\} \tag{6}$$

where $\mathbf{1}$ is a vector containing all 1 of length p and abs(.) is component-wise absolute value operation. An error occurs when $\mathbf{P}_{\hat{i}} \neq \mathbf{P}$. $\hat{i}$ is used to detect transmitted symbols by multiplying $\mathbf{P}_{\hat{i}}^T$ to $\tilde{\mathbf{y}}$,

$$\tilde{\mathbf{x}} = \mathbf{P}_{\hat{i}}^T\tilde{\mathbf{y}} = \mathbf{P}_{\hat{i}}^T\mathbf{\Lambda}\mathbf{P}\mathbf{\Lambda}\mathbf{s} + \mathbf{P}_{\hat{i}}^T\tilde{\mathbf{n}}. \tag{7}$$

Multiplying $\mathbf{P}_{\hat{i}}^T$ to $\tilde{\mathbf{y}}$ does not change the noise statistics since $\mathbf{P}_{\hat{i}}$ is a unitary matrix. Vector $\tilde{\mathbf{x}} = (\tilde{x}_j : j \in \{1, ..., p\})^T$ contains p elements to be demodulated as

$$\hat{s}_j = \min_x \left(\left\| \tilde{x}_j - x \right\|_2^2 \right), \; x \in \mathcal{S} \tag{8}$$

where $\|.\|_2$ is Euclidean norm. Finally, the detected $\hat{i}$ and $\{\hat{s}_1, \hat{s}_2, ..., \hat{s}_p\}$ are converted into bits.

C. Receiver Validity

Our receiver model shown in (6) can be verified using the following

$$(\mathbf{P}_i\mathbf{\Lambda}\mathbf{1})^T \mathrm{abs}(\mathbf{P}\mathbf{\Lambda}\mathbf{s}) \leq (\mathbf{P}\mathbf{\Lambda}\mathbf{1})^T \mathrm{abs}(\mathbf{P}\mathbf{\Lambda}\mathbf{s}), \quad \mathbf{P}_i, \mathbf{P} \in \mathcal{P} \tag{9}$$

where equality holds if and only if $\mathbf{P}_i = \mathbf{P}$, hence maximum is achieved when $\mathbf{P}_i = \mathbf{P}$. In other words, (6) is maximized when the input matrix $\mathbf{P}_i$ at receiver is equal to the selected $\mathbf{P}$ at the transmitter.

Theorem 1: receiver model (6) is valid if and only if absolute value of all elements in vector $\mathbf{s}$ are equal, $|s_1| = ... = |s_p|$.

Proof: Let $\mathbf{f}, \mathbf{g} \subseteq \mathbb{C}^p$, it dictates

$$\left| \mathbf{f}^T\mathbf{P}\mathbf{f}\mathbf{g}^T\mathbf{1} \right| \leq \left| \mathbf{f}^T\mathbf{I}\mathbf{f}\mathbf{g}^T\mathbf{1} \right|, \; \mathbf{P} \in \mathcal{P} \tag{10}$$

where $\mathbf{I}$ is identity matrix. When $\mathbf{g} = (g_1, ..., g_p : |g_1| = ... = |g_p|)$, equality holds when $\mathbf{P} = \mathbf{I}$. It implies that the upper bound is achieved when every element of vector $\mathbf{f}$ is multiplied with itself. This fact can be applied to (9) where the upper bound is achieved by choosing a permutation matrix such that each singular value is multiplied with itself. Therefore to comply this condition, vector $\mathbf{s}$ should satisfy $\mathbf{s} = (s_1, ..., s_p : |s_1| = ... = |s_p|)$, e.g., PSK modulation.

III. Capacity Analysis

A. Formal Derivation

We derive the capacity expression of PCM in this section. First, the mutual information of the proposed system is defined as

$$I(\mathbf{x}; \tilde{\mathbf{y}}) = H(\tilde{\mathbf{y}}) - H(\tilde{\mathbf{y}}|\mathbf{x}) \tag{11}$$

where $H(.)$ denotes the differential entropy. Capacity is obtained by choosing input distribution that maximize the mutual information in (11), then

$$C = \max_{f_\mathbf{x}} I(\mathbf{x}; \tilde{\mathbf{y}}) = \max_{f_\mathbf{x}} H(\tilde{\mathbf{y}}) - H(\tilde{\mathbf{y}}|\mathbf{x}). \tag{12}$$

It can be shown that

$$H(\tilde{\mathbf{y}}|\mathbf{x}) = \log_2 \det(\pi e \mathbf{K}_\mathbf{n}) \tag{13}$$

since perfect channel knowledge is known at transceiver and $\mathbf{n}$ and $\mathbf{x}$ are independent. Thus, the capacity computation in (12) is reduced to finding the input distribution on $\mathbf{x}$ to maximize $H(\tilde{\mathbf{y}})$. The fact that Gaussian distribution is a differential entropy maximizer. $H(\tilde{\mathbf{y}})$ is upper bounded by the entropy of a complex Gaussian random variable, hence C is maximized when $\tilde{\mathbf{y}} \sim \mathcal{CN}(0, \mathbf{K}_{\tilde{\mathbf{y}}})$. The entropy of $\tilde{\mathbf{y}}$ is computed as

$$H(\tilde{\mathbf{y}}) = \log_2 \det(\pi e \mathbf{K}_{\tilde{\mathbf{y}}}) \tag{14}$$

where $\mathbf{K}_{\tilde{\mathbf{y}}}$ is determined as

$$\mathbf{K}_{\tilde{\mathbf{y}}} = E[\tilde{\mathbf{y}}^2] = \mathbf{\Lambda}\mathbf{P}\mathbf{\Lambda}\mathbf{K}_\mathbf{x}\mathbf{\Lambda}\mathbf{P}^T\mathbf{\Lambda} + \mathbf{K}_\mathbf{n} \tag{15}$$

where $\mathbf{K}_\mathbf{x} = \mathrm{diag}(\gamma_1, ..., \gamma_p)^T$ is transmit symbol covariance matrix and γ_i is the i-th antenna transmit power. Note that due to uncorrelated noise, $\mathbf{K}_\mathbf{n} = \mathrm{diag}(\sigma_n^2, ..., \sigma_n^2)^T$ is a diagonal matrix containing noise variances. The channel is assumed to be fixed during the symbol duration, therefore the channel coefficient can be treated as constant. Substituting (13) and (14) to (12), we obtain

$$C = \log_2 \det \left(\mathbf{I} + \mathbf{\Lambda}\mathbf{P}\mathbf{\Lambda}\mathbf{K}_\mathbf{x}\mathbf{\Lambda}\mathbf{P}^T\mathbf{\Lambda}{\mathbf{K}_\mathbf{n}}^{-1} \right). \tag{16}$$

Note that $\left(\mathbf{I} + \mathbf{\Lambda}\mathbf{P}\mathbf{\Lambda}\mathbf{K}_\mathbf{x}\mathbf{\Lambda}\mathbf{P}^T\mathbf{\Lambda}\mathbf{K}_\mathbf{n}^{-1} \right)$ results in a diagonal matrix of size p where a pair of squared singular values are multiplied depends on the selected $\mathbf{P}$. It is convenient to define set of all possible singular values multiplication as $\mathcal{D} \in \{\zeta_1 = \lambda_1^2\lambda_1^2, \zeta_2 = \lambda_1^2\lambda_2^2, ..., \zeta_p = \lambda_p^2\lambda_p^2\}$. Now, (16) can be treated as summation over p channels as shown as below

$$C = \sum_{i=1}^{p} \log_2 \left(1 + \frac{\zeta_i \gamma_i}{\sigma_n^2} \right) \tag{17}$$

where $\zeta_i \in \mathcal{D}$. Note that $\zeta_i > 0 \; \forall i$ since λ_i is strictly positive.

B. Optimal Capacity

In this part, we discuss about the optimal capacity of PCM at each transmission. It is done by finding the optimal power allocation assigned to each transmit antenna at each transmission. The capacity is maximized by solving

$$\begin{aligned} \underset{\gamma_1,\ldots,\gamma_P}{\text{maximize}} \quad & \sum_{i=1}^{p} \log_2\left(1+\frac{\zeta_i\gamma_i}{\sigma_n^2}\right) \\ \text{subject to} \quad & \sum_{i=1}^{p}\gamma_i \le \Gamma, \qquad \gamma_i \ge 0 \ \forall i \end{aligned} \tag{18}$$

where Γ is total transmit power at each transmission. The objective function in (18) is concave since log(.) is concave. Therefore the optimization problem in (18) belongs to convex programming problems. Now, the proof relies on standard convex analysis and the constraints satisfy Slater's condition. Thus, the Karush-Kuhn-Tucker (KKT) condition is sufficient and necessary for optimality. By introducing dual variables ν and μ_i, the Lagrangian is formed as

$$L(\gamma_i,\nu,\mu_i) = -\sum_{i=1}^{p}\log_2\left(1+\frac{\zeta_i\gamma_i}{\sigma_n^2}\right) + \nu\left(\sum_{i=1}^{p}\gamma_i-\Gamma\right) - \sum_{i=1}^{p}\mu_i\gamma_i. \tag{19}$$

We derive the Lagrangian and the problem can be solved using the well-known water-filling (WF) algorithm. Optimal power allocation is computed as

$$\gamma_i = \max\left(\frac{1}{\nu}-\frac{\sigma_n^2}{\zeta_i},\ 0\right). \tag{20}$$

IV. Results and Discussion

In this section we present performance of PCM aiming to study the:

- capacity behavior of PCM with various antenna settings using equal and WF power allocation.
- capacity comparison to other existing techniques.
- outage probability in comparison to existing technique.
- BER of the detection scheme we proposed.

We conduct Monte Carlo simulation for all simulated results presented in this section. Capacity, outage probability and BER are all simulated in Rayleigh flat fading channel unless specified otherwise. For the sake of clarity, we separate this section into three subsections.

A. Capacity

We derive the capacity expression of PCM in (17). Monte Carlo simulation is used to average out the singular values. Further, standard Normal distribution is employed as the noise input.

Fig. 2 shows capacity performance of PCM with various antenna settings using equal power (EP) allocation and WF power allocation given in (20). WF shows better performance compared to EP for all antenna settings over all SNR range. It also shows that maximum achievable capacity can be attained via WF scenario. The same trends are shown by 4×4 and 7×7 settings as well as 4×7 and 7×4 settings. It implies that identical

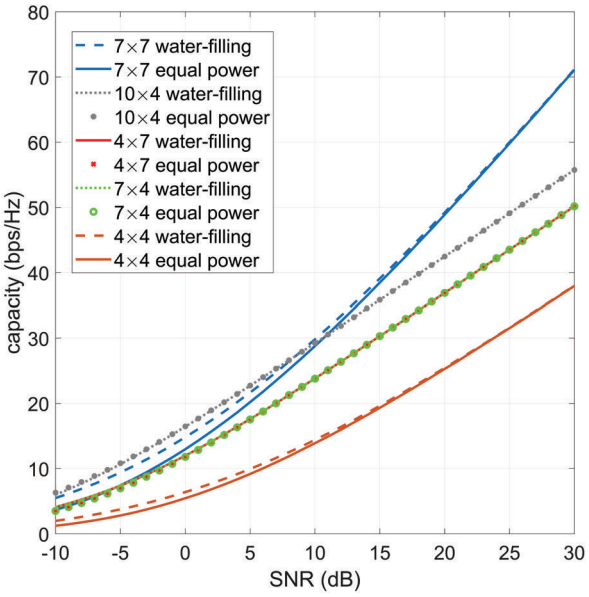

Fig. 2: Capacity of PCM

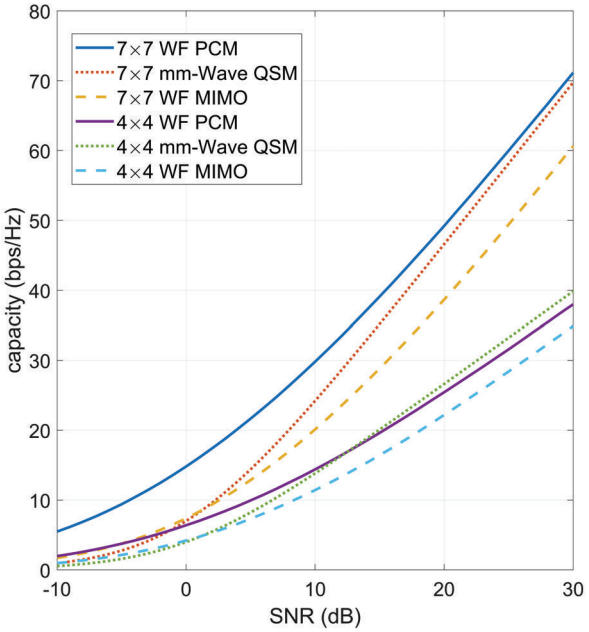

Fig. 3: Capacity comparison between WF PCM, WF MIMO and mmWave-QSM

antenna settings results identical capacity performances. Fig. 2 also represents that higher capacity can be obtained by increasing the channel rank of the system. However, different trend is shown by 10×4 setting. Although its channel rank is lower than 7×7 setting, it outperforms 7×7 setting in low SNR and declines in high SNR. This is due to the fact that 10×4 setting gains higher singular values than 7×7 setting. It can be observed from (16). The capacity is increased as the singular values ζ_i are increased. Furthermore, we can improve the singular values by increasing either the number of transmit or

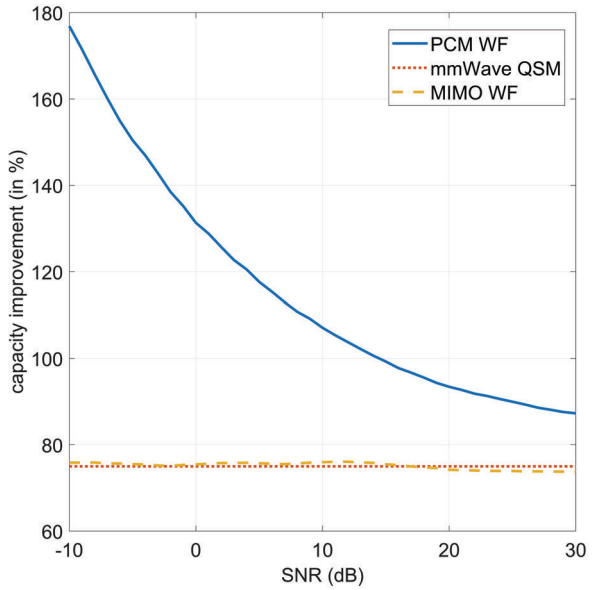

Fig. 4: Capacity improvement percentage of 4×4 to 7×7 of WF PCM, mmWave QSM and WF MIMO

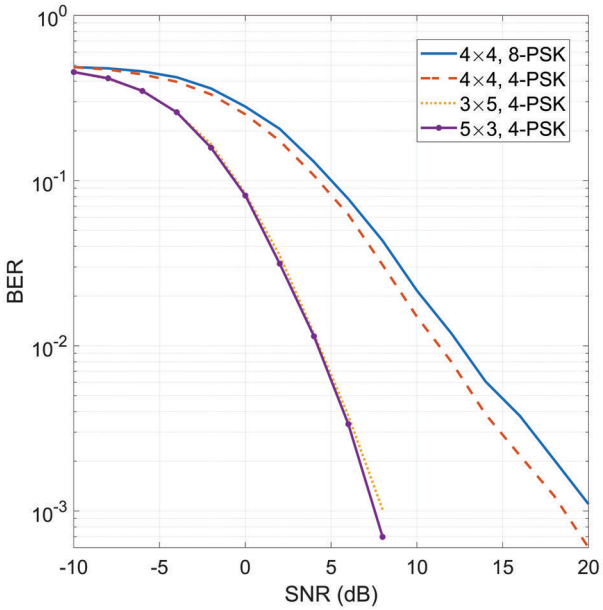

Fig. 6: BER of PCM

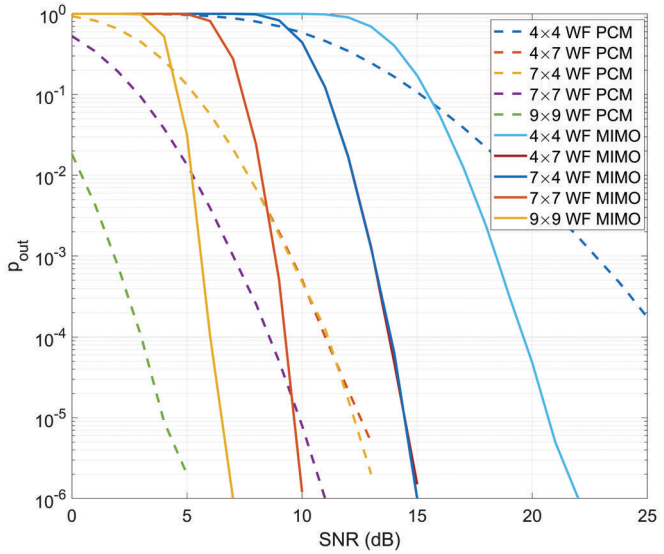

Fig. 5: Outage probability of WF PCM and WF MIMO with $R = 15$ bps/Hz

receive antennas [1]. On the other hand, increasing the channel rank p is also improving the capacity performance as shown in (16). We can also observe that increasing p is linear while increasing ζ_i is logarithmic to capacity C. Therefore, in the function of SNR, 10×4 and 7×7 settings are intersect at a point. In Fig. 2, we cover all possible antenna configuration scenarios. Thus, different values will result the same performance trend.

We compare PCM with other existing techniques in Fig. 3. WF power allocation is applied to both PCM and conventional MIMO. Time-invariant MIMO capacity is computed as

$$C_{\text{MIMO}} = \log_2 \det \left(\mathbf{I} + \mathbf{H}\mathbf{K}_{\mathbf{x}}\mathbf{H}^H \mathbf{K}_{\mathbf{n}}{}^{-1} \right) \tag{21}$$

where WF power allocation is employed over the diagonal matrix $\mathbf{K}_{\mathbf{x}}$. We also compare PCM to QSM as one of the most recently developed space modulation techniques. Furthermore, QSM has been successfully extended to work in mmWave channel as shown in [12]. The closed-form capacity expression in 3D mmWave channel has also been derived and can be computed as

$$C_{\text{QSM}} = M \log_2 \left(1 + \frac{1}{\sigma_n^2} \right). \tag{22}$$

As shown in Fig. 3, higher antenna setting gives more capacity improvement for all techniques over whole SNR range. WF MIMO lies below WF PCM at both 7×7 and 4×4 settings. PCM attains 103% to 9% capacity gain using 4×4 setting and 220% to 17% capacity gain using 7×7 setting compared to WF MIMO over 0 to 30 dB. By increasing the channel rank from $p = 4$ to $p = 7$, WF PCM doubles the percentage gap over WF MIMO. It also implies that PCM is getting higher singular values compared to MIMO as intuitively can be observed in (16) and (21). On the other hand, PCM and mmWave QSM curves are intersect at certain SNR values. PCM is superior to mmWave QSM prior to the intersection and the opposite occurs afterwards. Capacity of mmWave QSM is M times Gaussian noise capacity due to the absence of channel gain.

In Fig. 4, we calculate the percentage of capacity improvement of 4×4 to 7×7 setting by taking their ratio over the whole SNR range. It shows that mmWave QSM and WF MIMO improve around 78% over the whole SNR range. While WF PCM varies from 176% to 87%. It implies that WF PCM can improve higher capacity by increasing the antenna settings than mmWave QSM and WF MIMO.

Findings: *1) Maximum achievable capacity of PCM can be acquired using WF scenario. 2) Despite the same channel rank,*

capacity can be increased by adding either transmit or receive antenna in PCM. 3) PCM can improve the capacity better by increasing the channel rank than MIMO and mmWave QSM.

B. Outage Probability

Outage probability is defined as the probability that information rate being below the required threshold. In general, outage probability is computed as

$$p_{\text{out}} = \text{P}\{C < R\}, \tag{23}$$

where R is information rate threshold. We present the outage probability of WF PCM and WF MIMO in Fig. 5 with $R = 15$ bps/Hz. The results are different in different settings. PCM with 4×4 setting lies above 10^{-4} at 25 dB while MIMO only requires around 19.5 dB to achieve the same outage probability with same antenna settings. However, the performance of PCM improves more than MIMO for increased number of antennas. An interesting fact is shown by 4×7 and 7×4 curves. The performances are overlapped for both settings where PCM outperforms MIMO over the SNR range. It implies that PCM achieves more improvement than MIMO by either increasing transmit or receive antennas or both. In other words, PCM is able to reduce the outage probability better than MIMO. Finally, we can observe that 9×9 setting of PCM obtains the best result where at 0 dB the probability is close to 10^{-2} while MIMO requires around 4.8 dB to achieve the same probability.

Findings: *1) PCM's outage probability increases dramatically by increasing either number of transmit or receive antenna or both. 2) PCM is superior to MIMO in high number of antenna setting.*

C. BER

We present the BER of PCM in Fig. 6 with different configurations. The 3×5 and 5×3 4-PSK settings are overlapped over the SNR range. Despite the difference of number of transmit and receive antennas, same channel rank and PSK level deliver identical results. On the other hand, different channel rank with same PSK level shows distinct performance as shown by 3×5 and 4×4 4-PSK. Different PSK level with same antenna setting is also presented. Higher level causes poorer BER. We can also observe that increasing channel rank gives worse BER than increasing PSK level.

Findings: *1) The higher the channel rank or PSK level, the poorer the performance. 2) Enhancing channel rank affects the BER worse than increasing PSK level.*

V. Conclusions and Future Work

We propose a novel index modulation mechanism called PCM by exploiting the spatial resource of MIMO. Capacity expression is derived and compared with MIMO and mmWave QSM. The results show PCM has better performance over the compared techniques. We also define optimal water-filling power allocation for PCM to obtain maximum achievable capacity. Comparison of performance with WF MIMO represents that WF PCM outperforms WF MIMO. We also evaluate our work by providing outage probability in comparison with WF MIMO. PCM is able to reduce the outage probability better than MIMO by increasing either transmit or receive antennas or both. Finally, we discuss BER of PCM with various antenna settings and modulation levels to analyze our detection scheme. It indicates the increase of channel rank gives worse performance than the increase of modulation level.

We will expand the advantages offered by PCM in future works as well as analyze system complexity and further develop a detection scheme that works in general, i.e., QAM.

Acknowledgment

This work has been financially supported in part by the 6Genesis (6G) Flagship project (grant 318927).

References

[1] G. Lebrun, J. Gao, and M. Faulkner, "Mimo transmission over a time-varying channel using svd," *IEEE Transactions on Wireless Communications*, vol. 4, no. 2, pp. 757–764, 2005.

[2] C. Wang, X. Hong, X. Ge, X. Cheng, G. Zhang, and J. Thompson, "Cooperative mimo channel models: A survey," *IEEE Communications Magazine*, vol. 48, no. 2, pp. 80–87, 2010.

[3] K. Zheng, L. Zhao, J. Mei, B. Shao, W. Xiang, and L. Hanzo, "Survey of large-scale mimo systems," *IEEE Communications Surveys Tutorials*, vol. 17, no. 3, pp. 1738–1760, 2015.

[4] F. W. Murti, R. F. Siregar, and S. Y. Shin, "Su-mimo based uplink non-orthogonal multiple access for 5g," *Journal of Network and Computer Applications*, vol. 110, pp. 87 – 96, 2018. [Online]. Available: http://www.sciencedirect.com/science/article/pii/S1084804518300900

[5] R. Y. Mesleh, H. Haas, S. Sinanovic, C. W. Ahn, and S. Yun, "Spatial modulation," *IEEE Transactions on Vehicular Technology*, vol. 57, no. 4, pp. 2228–2241, July 2008.

[6] R. F. Siregar, F. W. Murti, and S. Y. Shin, "Bit allocation approach of spatial modulation for multi-user scenario," *Journal of Network and Computer Applications*, vol. 127, pp. 1 – 8, 2019.

[7] I. Lai, J. Shih, C. Lee, H. Tu, J. Chi, J. Wu, and Y. Huang, "Spatial permutation modulation for multiple-input multiple-output (mimo) systems," *IEEE Access*, vol. 7, pp. 68 206–68 218, 2019.

[8] R. F. Siregar, F. W. Murti, and S. Y. Shin, "Combination of spatial modulation and non-orthogonal multiple access using hybrid detection scheme," in *2017 Ninth International Conference on Ubiquitous and Future Networks (ICUFN)*, 2017, pp. 476–481.

[9] R. Mesleh, S. S. Ikki, and H. M. Aggoune, "Quadrature spatial modulation," *IEEE Transactions on Vehicular Technology*, vol. 64, no. 6, pp. 2738–2742, June 2015.

[10] R. F. Siregar, N. Rajatheva, and M. Latva-aho, "Qsm based noma for multi-user wireless communication," in *2019 16th International Symposium on Wireless Communication Systems (ISWCS)*, Aug 2019, pp. 139–144.

[11] R. Mesleh, S. Althunibat, and A. Younis, "Differential quadrature spatial modulation," *IEEE Transactions on Communications*, vol. 65, no. 9, pp. 3810–3817, Sept 2017.

[12] A. Younis, N. Abuzgaia, R. Mesleh, and H. Haas, "Quadrature spatial modulation for 5g outdoor millimeterwave communications: Capacity analysis," *IEEE Transactions on Wireless Communications*, vol. 16, no. 5, pp. 2882–2890, 2017.

[13] S. Guo, H. Zhang, P. Zhang, S. Dang, C. Liang, and M. Alouini, "Signal shaping for generalized spatial modulation and generalized quadrature spatial modulation," *IEEE Transactions on Wireless Communications*, vol. 18, no. 8, pp. 4047–4059, 2019.

[14] M. Wen, B. Zheng, K. J. Kim, M. Di Renzo, T. A. Tsiftsis, K. Chen, and N. Al-Dhahir, "A survey on spatial modulation in emerging wireless systems: Research progresses and applications," *IEEE Journal on Selected Areas in Communications*, vol. 37, no. 9, pp. 1949–1972, 2019.

[15] A. Younis, N. Serafimovski, R. Mesleh, and H. Haas, "Generalised spatial modulation," in *2010 Conference Record of the Forty Fourth Asilomar Conference on Signals, Systems and Computers*, 2010, pp. 1498–1502.

[16] G. Lebrun, J. Gao, and M. Faulkner, "Mimo transmission over a time-varying channel using svd," *IEEE Transactions on Wireless Communications*, vol. 4, no. 2, pp. 757–764, 2005.